Problem Chosen	2026 MCM/ICM Summary Sheet	Team Control Number
A		2618558

Input Your Article Title Here if it is too Long

Summary

This is abstract.This section should describe what problem the paper solves, what methods are applied, what results are obtained and summarize them.

This is the second line abstract.And if you look carefully you can see that the spacing within and between paragraphs is different, which facilitates our reading in paragraphs.

This is **the** special `special` *special* *special* fonts in abstract.

Keywords: Fighting Wildfires; Multi-Objective Optimization; Poisson Distribution; Tabu Search Algorithm; Sensitivity Analysis

Contents

1 Ideal Battery

1.1 Assumptions

To consider an simplist ideal battery model, the following assumptions are made:

- The battery is kept at a constant environment, so the temperature effects are neglected.
- The battery has no energy loss during charging and discharging.
- The battery has infinite cycle life, so the degradation effects are neglected and all the parameters are constant.
- The Open Circuit Voltage (OCV) is only related to the SoC, so we can express the SoC as a functionof U_{OC}:
$$SoC = f(U_{OC}) \tag{1}$$
in which $f(\cdot)$ can be obtained through curve fitting based on experimental data.
- The battery behavior is same for charging and discharging. For smartphones, which mostly use $LiCoO_2$ batteries that has little or no hysteresis, this assumption is reasonable.

1.2 Thevenin Model

A Li-ion battery system can be extremely complex, involving electrochemical, thermal and mechanical processes. However, for system-level studies, an equivalent circuit model is often used to represent the battery behavior. The Thevenin model is a widely used equivalent circuit model that captures the dynamic response of the battery voltage during charge and discharge cycles. The model is described as follows:

The relationship between U_{OC} and other parameters in the Thevenin model can be expressed with Kirchhoff's laws:

$$U_{OC} = U_t + IR_0 + U_1 + U_2 \tag{2}$$

in which U_t is the terminal voltage.

For U_1, U_2 we have:

$$I = C_1\frac{\mathrm{d}U_1}{\mathrm{d}t} + \frac{U_1}{R_1} = C_2\frac{\mathrm{d}U_2}{\mathrm{d}t} + \frac{U_2}{R_2} \tag{3}$$

Differentiateing the SoC's definition with respect to time, we get:

$$\frac{\mathrm{d}(SoC)}{\mathrm{d}t} = -\frac{I}{Q_{max}} \tag{4}$$

where Q_{max} is the maximum capacity of the battery.

Combining the above equations, we can derive the complete Thevenin model in matrix form:

$$\frac{\mathrm{d}}{\mathrm{d}t}\begin{bmatrix} SoC \\ U_1 \\ U_2 \end{bmatrix} = \begin{bmatrix} 0 & 0 & 0 \\ 0 & -\frac{1}{R_1C_1} & 0 \\ 0 & 0 & -\frac{1}{R_2C_2} \end{bmatrix}\begin{bmatrix} SoC \\ U_1 \\ U_2 \end{bmatrix} + \begin{bmatrix} -\frac{1}{Q_{max}} \\ \frac{1}{C_1} \\ \frac{1}{C_2} \end{bmatrix} I \tag{5}$$

where $R_0, R_1, R_2, C_1, C_2, Q_{max}$ are the model parameters that need to be estimated.

1.3 Parameter Estimation

The Hybrid Pulse Power Characterization (HPPC) test is commonly used for this purpose. The test is conducted with steps as follows:

1. The battery is first fully charged to 100% SoC in ways the manufacturer recommends.
2. After resting for a certain period(e.g. 1 hour), the battery is discharged with a constant current pulse (e.g., $0.5C$) for a short duration (e.g., $10s$). The voltage response is recorded.
3. Then discharge the battery to another selected SoC point (e.g., 90%).
4. Repeat steps 2 and 3 until the battery reaches a low SoC point (e.g., 10%) or the maximum discharge limit the manufacturer specifies.
5. If needed, repeat similar steps for charging pulses.

With HPPC data, the model parameters can be estimated through curve fitting techniques. The process are as follows:

- **Estimate** R_0: The instantaneous voltage drop at the start of each pulse can be used to estimate the internal resistance R_0, at which point the capacitive effects are negligible.
$$R_0 = \frac{\Delta U_{instant}}{I_{pulse}} \tag{6}$$
- **Estimate** R_1, C_1 **and** R_2, C_2: Solve the polarization equation (3), we can get the polarization voltage response:
$$U_{polar} = IR + (U_{init} - IR)e^{-\frac{t}{RC}} \tag{7}$$
where U_{init} is the voltage at the start of the pulse.
Without loss of generality, let $R_1C_1 \leq R_2C_2$, so that the faster electrochemical polarization are represented by R_1, C_1 and the slower concentration polarization effects are represented by R_2, C_2. Then substitute them into (2), we have:
$$U_t = U_{OC} - I(R_0 + R_1 + R_2) - (U_{1,init} - IR_1)e^{-\frac{t}{R_1C_1}} - (U_{2,init} - IR_2)e^{-\frac{t}{R_2C_2}} \tag{8}$$
By least squares fitting of (8) to the voltage response data during each pulse, we can estimate the values of R_1, C_1 and R_2, C_2 at different SoC points.
- **Estimate** Q_{max}: The maximum capacity Q_{max} can be estimated by integrating the current over the full discharge cycle:
$$Q_{max} = \int_{t_0}^{t_f} I(t)\mathrm{d}t \tag{9}$$
where t_0 and t_f are the start and end times of the discharge cycle.
Most of the time this value is provided by the manufacturer.

We use a Samsung INR21700 30T 3Ah Li-ion Battery Dataset to demonstrate the parameter estimation process. The fitting result are shown as follows:

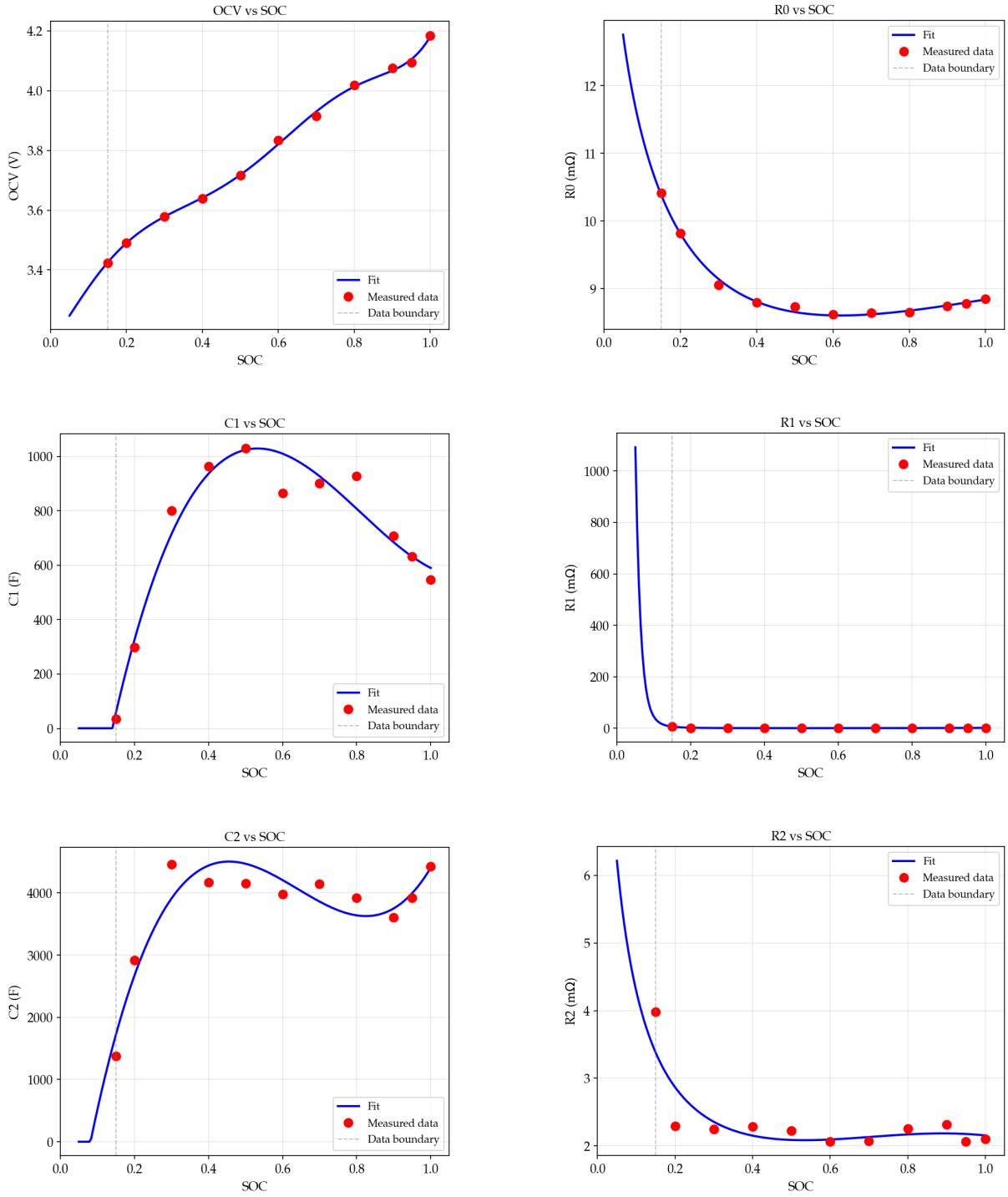

Figure 1: Fitting results of the parameter estimation process.

6-degree polynomial is used to fit the OCV-SOC curve, cubic functions are used to fit the C_1, C_2, and double exponential functions $y = A_1 e^{B_1 x} + A_2 e^{B_2 x} + C$ are used to fit the R_0, R_1, R_2 curves.

As the fitting result shows, the Ohm resistance R_0 increases significantly when SoC is low, which may be the main reason for voltage drop and device shutdown. Later we will verify this conclusion. Polarization resistances R_1, R_2 also increase when SoC

is low, indicating the battery's internal electrochemical processes are hindered. And Polarization capacitances C_1, C_2 decrease when SoC is low, meaning that the battery's ability to respond to load changes is weakened.

Noticed that C_1, C_2 drop to zero when SoC is low, which means the Thevenin model is not valid in that region. However, the smartphone will actually shutdown before the battery reaches such low SoC, because the output voltage will be too low to power the device.

1.4 Simulations

With proper model parameters, we can do numerical simulations of the battery behavior under different load profiles. 2 simplified load profiles are considered here:

- Constant current;
- Constant power.

1.4.1 Constant current

Since the current is constant, equation (4) can be directly integrated to get the SoC at time t:

$$SoC(t) = SoC(0) - \frac{It}{Q_{max}} \tag{10}$$

Then perform Rk45 algorithm to the polarization voltages U_1, U_2 with initial conditions $U_1(0) = U_2(0) = 0$, we can get the final result as follows.

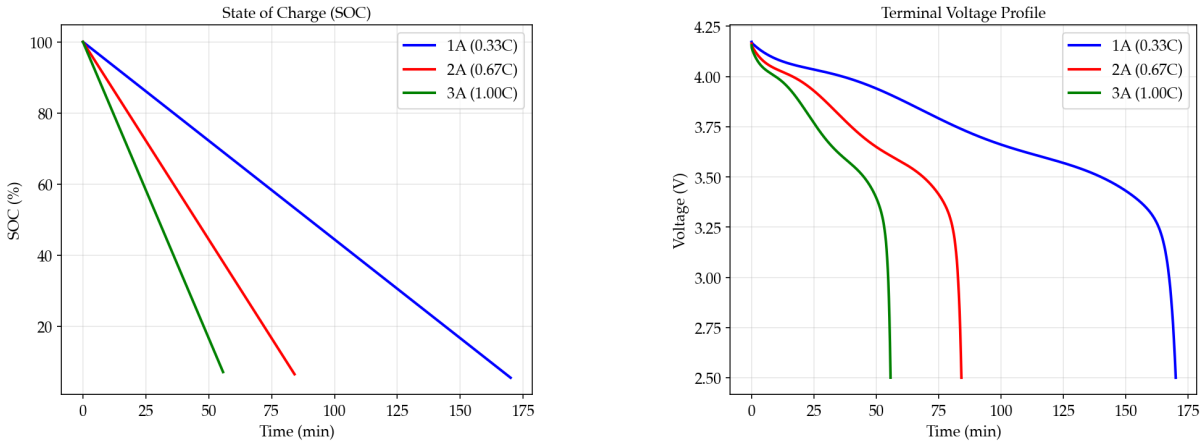

Figure 2: Simulation results under constant current load profile

It can be seen that although the SoC decreases linearly under constant current load, the terminal voltage decreases steadily at first, then suddenly drops to a "dead" value, which makes the device shutdown. The phenomenon is consistent with our daily experience.

1.4.2 Constant power

The output power

$$P = U_t I \tag{11}$$

is constant. In this case, analytic solutions are impossible, so we just use the Rk45 algorithm:

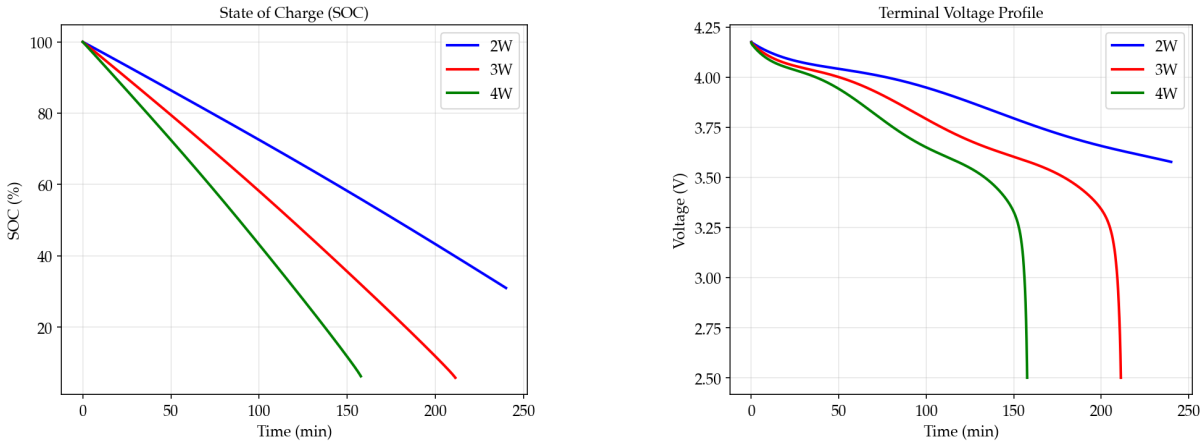

Figure 3: Simulation results under constant power load profile

Similar phenomena can be observed under constant power load profile. However, the terminal voltage drops more rapidly compared to the constant current case, indicating that constant power loads are more stressful to the battery.

2 Actual Battery

2.1 Assumptions

An actual battery is much more complex than the idealized model presented in the previous section. In this section, we will consider more factors that affect the performance and behavior of real batteries:

- **Temperature**: The performance of a battery can vary significantly with temperature. At low temperatures, the internal resistance increases, leading to reduced capacity and power output. Conversely, high temperatures can enhance performance but may also accelerate degradation.
- **Complex Power Profile**: Real batteries often experience varying power demands, which can affect their efficiency and lifespan. High performance demands can lead to increased heat generation, which int turns affect battery temperature.
- **Shutdown Voltage**: Electronics need a minimum voltage to operate correctly. If the battery voltage drops(steadily or suddenly) below this threshold, the device will shutdown even if SoC is not zero. In this section, we'll assume that if the battery voltage drops below 3.2V, the device will shutdown immediately.

2.2 Temperature Behavior of Battery

Actual battery behavior is significantly influenced by temperature variations. The most common parameter affected by temperature is the internal resistance. Using the Arrhenius' equation, we can model the temperature dependence of internal resistance as follows:

$$R = R_0 \cdot e^{\frac{E_a}{R_u T}} \tag{12}$$

where R_0 is a reference resistance, E_a is the activation energy, R_u is the universal gas constant and T_0 is a reference temperature.

To conduct the regression, rewrite the equation in linear form by taking the natural logarithm:

$$\ln R = \frac{E_a}{R_u} \cdot \frac{1}{T} + \ln R_0 \tag{13}$$

The Samsung INR21700 30T 3Ah Li-ion Battery Dataset contains experimental data at various temperatures. Using this dataset again, we perform a linear regression, yielding the following results:

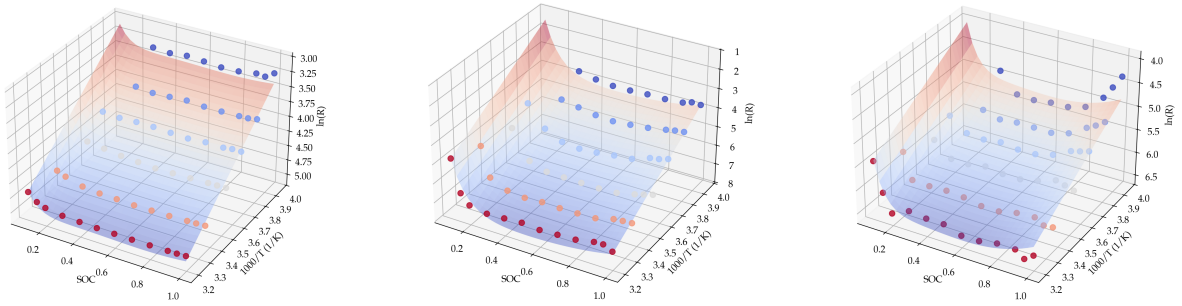

(a) R_0, $E_a = 17.47kJ/mol$ (b) R_1, $E_a = 37.24kJ/mol$ (c) R_2, $E_a = 15.09kJ/mol$

Figure 4: 3D Surface Fitting of Resistance with Temperature and SoC

If we consider the temperature effect, the simulation heatmap of discharge time from 100% SoC under different power load and temperature will be as follows:

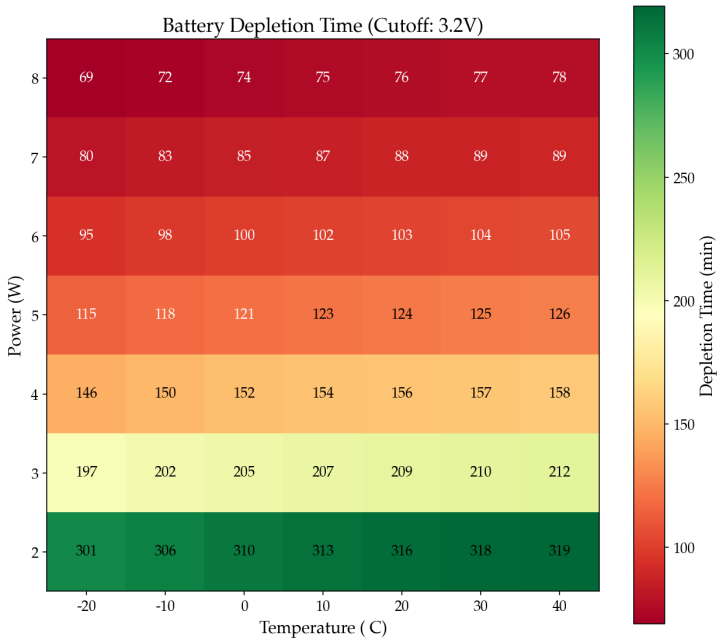

Figure 5: Heatmap of Discharge Time with Power Load and Temperature

It can be observed that battery behaves badly at low temperatures, and the discharge time decreases significantly as temperature drops. However, although high temperature improves battery short-term performance, it also accelerates battery degradation over time. Therefore, in practical applications, maintaining an optimal temperature range is crucial for battery longevity and performance.

2.3 Battery in Different Work Loads

A smartphone is a complex embedded system whose total power consumption can be decomposed into the sum of contributions from its independent subsystems. According to the **Principle of Power Superposition**, when individual modules share a power supply but operate relatively independently, the total power draw can be expressed as a linear superposition of the power consumption of each module.

Based on a functional module breakdown, we decompose the smartphone's power consumption into the following six primary sources:

- **Display Screen**: Backlight/OLED driver
- **CPU Computation**: Processor dynamic power
- **Network Communication**: WiFi/Cellular radio frequency (RF)
- **Location Service**: GPS reception and computation
- **Audio Playback**: Codec and speaker driver
- **System Mode**: Adjustment effects from power-saving/flight modes

Overall, the model can be written as:

$$\boxed{P_{\text{total}} = P_{\text{screen}} + P_{\text{CPU}} + P_{\text{network}} + P_{\text{GPS}} + P_{\text{audio}} + P_{\text{mode}}} \tag{14}$$

In this section, we will develop physical models for each component. By utilizing acquired smartphone state data, we estimate the parameters within these models, thereby obtaining a comprehensive power consumption model for complex usage scenarios.

2.3.1 Screen Power P_{screen}

When the screen is on, it exhibits a base power draw plus a near-linear OLED power component (the modeling here assumes an OLED display):

$$P_{\text{screen}} = \alpha_S \cdot S + \alpha_B \cdot S \cdot \frac{B}{255} \tag{15}$$

where S is a screen state indicator and B is the brightness level (0–255).

2.3.2 CPU Power P_{CPU}

CPU power is the largest variable power source in a smartphone. According to the dynamic power formula for CMOS circuits:

$$P_{\text{dynamic}} = C \cdot V^2 \cdot f \tag{16}$$

where C is the load capacitance, V the operating voltage, and f the clock frequency.

Modern processors employ **Dynamic Voltage and Frequency Scaling (DVFS)**, introducing a coupling between voltage and frequency. Empirical studies suggest:

$$V \propto f^{0.5} \quad \Rightarrow \quad P \propto f^{2.5} \tag{17}$$

Furthermore, modern ARM processors commonly adopt a **big.LITTLE heterogeneous architecture**, featuring separate big and small cores with distinct performance and power characteristics. Additionally, actual CPU power depends on its utilization; idle and fully loaded states at the same frequency exhibit significantly different power draws. Thus, we derive the following CPU power model:

$$P_{\text{CPU}} = \alpha_U \cdot U + \alpha_{\text{big}} \cdot \left(\frac{f_{\text{big}}}{f_{\text{max,big}}} \right)^{2.5} + \alpha_{\text{small}} \cdot \left(\frac{f_{\text{small}}}{f_{\text{max,small}}} \right)^{2.5} \tag{18}$$

where U represents CPU utilization, and f_{big}, f_{small} are the operating frequencies of the big and small cores, normalized to their respective maximum frequencies.

2.3.3 Network Power P_{network}

Power consumption in wireless communication stems primarily from the Radio Frequency (RF) front-end, especially the Power Amplifier (PA). According to the Friis transmission equation, received power is inversely proportional to the square of the distance:

$$P_r = P_t \cdot G_t \cdot G_r \cdot \left(\frac{\lambda}{4\pi d} \right)^2 \tag{19}$$

Consequently, to maintain communication quality over distances up to several kilometers for cellular networks, relatively high transmit power is required (typically 200–500 mW). In contrast, WiFi communication with a router within tens of meters uses lower transmit power (typically 50–100 mW). Moreover, PA efficiency is typically only 30–40%, with substantial energy converted to heat, making network power a significant contributor to total consumption.

Since WiFi and cellular networks are typically used exclusively in practice, our model uses a single indicator variable for network type:

$$P_{\text{network}} = \alpha_M \cdot M \tag{20}$$

where M indicates active network type.

2.3.4 GPS Power P_{GPS}

The GPS module continuously receives weak signals from multiple satellites and performs complex signal demodulation and position calculation. Its power draw is relatively stable and depends mainly on whether it is active. We adopt a discrete model:

$$P_{\text{GPS}} = \alpha_G \cdot G \tag{21}$$

where G is a binary indicator for GPS activity.

2.3.5 Audio Power P_{audio}

The audio module primarily involves compression/decompression processing via an audio DSP, digital-to-analog conversion (DAC), and driving speakers or headphones. We simplify the modeling to a binary indicator for audio playback activity:

$$P_{\text{audio}} = \alpha_A \cdot A \tag{22}$$

2.3.6 System Mode Power Adjustment P_{mode}

Modern smartphones offer various system modes for power management, such as Power Saving Mode and Flight Mode. However, most of their energy-saving effects are achieved by altering other parameters (e.g., reducing CPU frequency, limiting network activity), which are already captured by other terms in the model. Therefore, P_{mode} represents additional energy-saving mechanisms. Power Saving Mode may disable unnecessary sensors, reduce refresh rates, and optimize memory management, while Flight Mode directly powers down RF modules. The model is:

$$P_{\text{mode}} = \alpha_E \cdot E + \alpha_F \cdot F \tag{23}$$

where E and F are indicators for Power Saving Mode and Flight Mode, respectively. Expectedly, $\alpha_E \leq 0$ and $\alpha_F \leq 0$.

2.3.7 Parameter Estimation and Validation

We performed physically constrained regression using the L-BFGS-B optimizer on normalized and binarized data, enforcing non-negative coefficients for power components and non-positive coefficients for power-saving modes. Substituting the estimated parameters yields the final empirical model:

$$\boxed{\begin{aligned} P_{\text{total}} = 0.250S + 0.615S\frac{B}{255} + 0.860U + 1.125f_{\text{big}}^{2.5} + 0.650f_{\text{small}}^{2.5} \\ + 0.696M + 0.040G + 0.397A - 0.068E - 0.028F \end{aligned}} \tag{24}$$

Subsequently, we can analyze the contribution rate of each parameter and evaluate the model's performance.

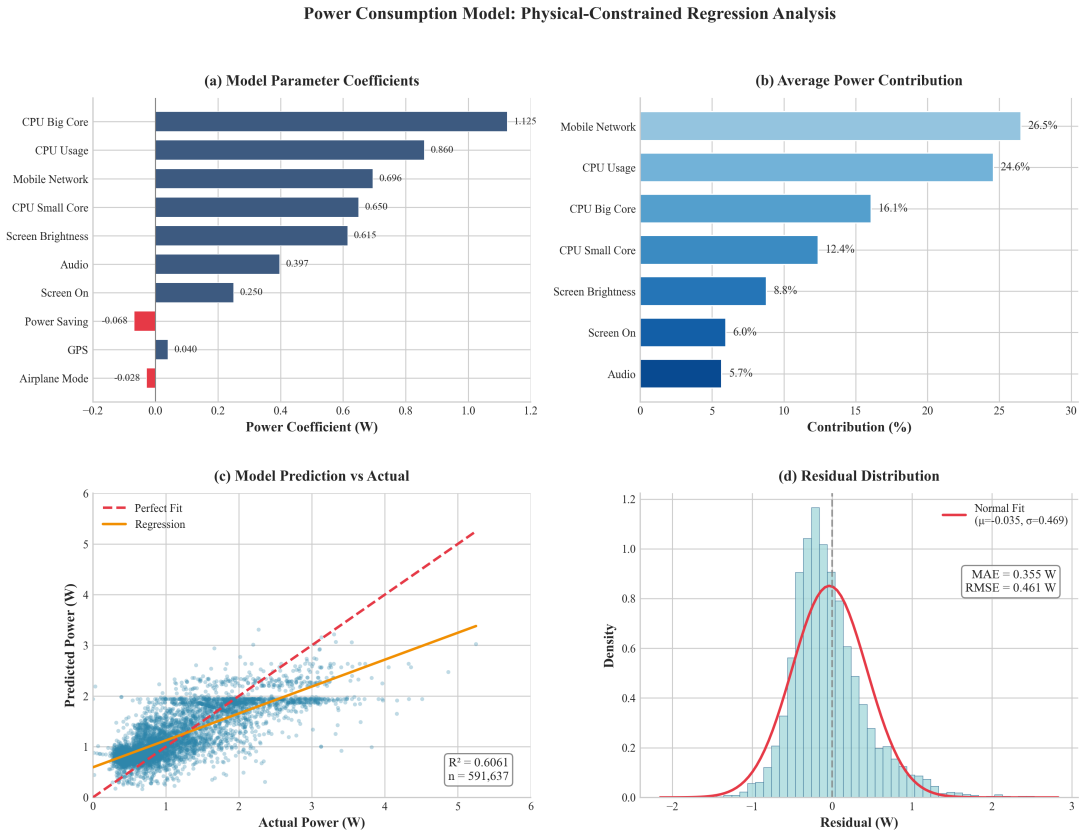

Figure 6: Model fitting results and parameter contribution analysis

2.3.8 Usage Scenario Simulation

The model allows us to estimate the smartphone's power consumption under various typical usage scenarios.

Power Consumption Under Different Usage Scenarios

Scenario	Screen (S)	Brightness (B/255)	CPU Usage	Big Core Freq	Small Core Freq	Mobile Network	GPS	Audio	Total Power (W)
Standby	Off	0%	10%	10%	10%	No	Off	Off	**0.09**
Web Browsing	On	50%	50%	30%	30%	No	Off	Off	**1.08**
Video Streaming	On	71%	40%	40%	30%	No	Off	On	**1.57**
Navigation	On	100%	50%	50%	40%	Yes	On	On	**2.69**
Gaming	On	100%	90%	100%	100%	Yes	Off	On	**4.51**

Figure 7: Power consumption under different usage scenarios

2.4 Heat Transfer Model in High-Performance Scenarios

In this chapter, we discuss how the heat that battery generates affacts the temperature of battery itself, and in turn impacts its own performance.

Let Q be the internal heat power, h be the convective heat transfer coefficient, A be the surface area of the battery(assumed to be the area of the smartphone), C be the heat capacity of the battery, T be the battery temperature and T_{env} be the environmental temperature(assumed constant). With Newton's law of cooling, we have:

$$Q = 2Ah(T - T_{env}) + C\frac{dT}{dt} \tag{25}$$

Q can be divided to:

$$Q = Q_{battery} + Q_{processor} + Q_{other} \tag{26}$$

$Q_{battery}$ can be further expressed with the Joule's law:

$$Q_{battery} = I^2 R_{inter} = I^2(R_0 + R_1 + R_2) \tag{27}$$

$Q_{processor}$ often is the major part of heat generation, because processors are often energy-intensive and almost all consumed energy is converted to heat. Here we model $Q_{processor}$ as a part of total power consumption of the device:

$$Q_{processor} = \eta P_{total} \tag{28}$$

in which η is some coefficient.

And the other components' heat generation Q_{other} can be assumed to be a constant for simplicity.

Considering that I and R is time-dependent, equation (25) is a first-order linear ODE. The solution is:

$$T = T_{env} + \frac{1}{C}\int_0^t e^{-\frac{2Ah(t-s)}{C}} Q(s)\mathrm{d}s \tag{29}$$

Substitute equation (29) into the Arrhenius' equation, we can get the relation between internal resistance and time, and thus analyze how temperature affects battery performance over time in high-performance scenarios.

The simulation here shows the heatmap of discharge time and max temperature under different power load and environmental temperature. It assumes if the battery temperature exceeds $50°\mathrm{C}$, the device will shutdown to protect the battery. In reality, smartphones often decreases processor frequency to reduce heat generation when temperature is too high, but for simplicity we assume an immediate shutdown here.

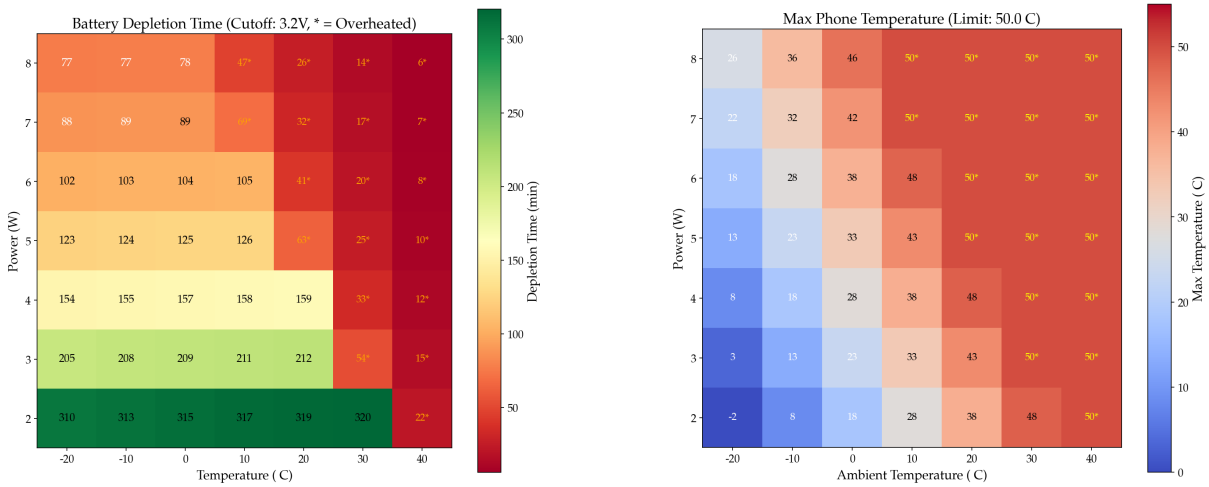

Figure 8: Heatmap of Discharge Time and Max Temperature

In the simulation we set $C = 160\text{J/K}$, $A = 200\text{cm}^2$, $h = 5\text{W}/(\text{m}^2 \cdot \text{K})$, $\eta = 0.5$ and $Q_{other} = 0.8\text{W}$.

It can be observed that high temperature scenarios are quite dangerous for battery operation. Heavy work loads in $30°\text{C}$ or higher can easily lead to battery overheating.

2.5 Answer to Question 1

2.6 Answer to Question 2